

PRACTICAL METHOD FOR DYNAMIC INTERACTION ANALYSIS OF
THREE-DIMENSIONAL DAM-FOUNDATION SYSTEM

T. OHMACHI (I)

S. SOGA (II)

Presenting Author: T. OHMACHI

SUMMARY

A simplified method for dynamic analysis of earth dam with foundation interaction is presented for practical application. It reduces a three dimensional dam-foundation system to a series of two degrees of freedom system connected along the dam axis, representing the dam as an assemblage of prismatic finite element, and employing the concept of the dynamical ground compliance. After a demonstration of the dam-foundation interaction observed by micro-tremor measurements, formulation of the method is described with analytical examples.

INTRODUCTION

It has been well known that an actual embankment dam especially built in a narrow canyon would reveal significant influence of canyon restraint on its vibration characteristics during earthquakes. Moreover, not a few earthquake records obtained simultaneously at both abutments of existing dams have shown differences in amplitude as well as in phase (Ref.1). Thus, dynamic analysis of an actual dam should take into account these three-dimensional effects in an appropriate manner. On this basis, the authors proposed a simplified three-dimensional finite element model which has proved to give satisfactory results for practical purposes (Réfs. 2, 3). In this article, the simplified model is extended to a dam-foundation system.

Due to the facts that ideal construction sites for higher dams have become small in number, and that embankment dams are adaptable to relatively poor dams sites, the dynamic interactions with embankment dam and foundation seem to be one of the most important subjects to secure earthquake resistance of dam. With an extremely large computational job and tedious work, the dynamic dam-foundation interaction in three-dimension could be treated by applying the finite element technique developed for the two-dimensional system (Ref. 4). The simplified method presented here is aiming at improvement of the practical applicability. Prior to formulation of the method, an instance of the interaction observed at an actual large dam is briefly shown.

INTERACTION CHARACTERISTICS OBSERVED AT AN ROCKFILL DAM

Micro-tremor measurements were carried out at an existing rockfill dam which is 90 m high and 487 m long on the crest. The left bankside of the dam is founded on uncemented deposits mainly of volcanic mud flows by which basement rock of hard dacite is thickly covered, as shown in Fig. 1. In the figure are shown typical Fourier amplitude spectra at several observation

(I) Associate Professor, The Graduate School at Nagatsuta, Tokyo Institute of Technology, Yokohama, Japan

(II) Graduate Student, ditto

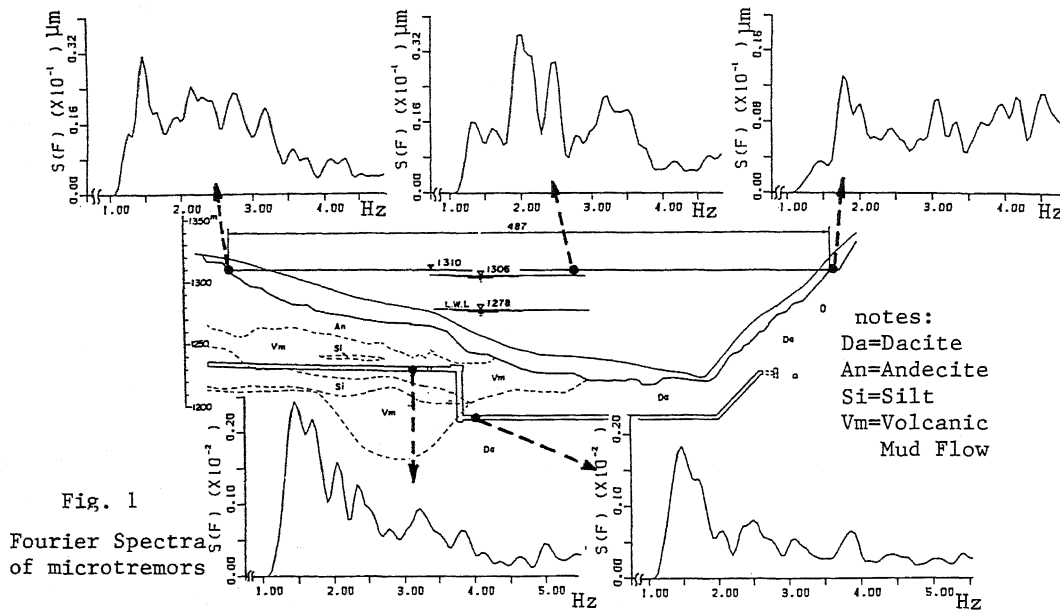


Fig. 1
 Fourier Spectra
 of microtremors

points. It can be seen that the displacement amplitude of the left abutment is almost twice as large as that of the right abutment, and that a lot of peak frequencies are too close to each other to distinguish natural vibration modes.

FORMULATION OF THE METHOD

Simplified 3-D Finite Element Modeling of Dam

Let us take the x-coordinate parallel to the axis of a dam, y- in the upstream-downstream direction, and z- vertically downward. Basic assumptions employed in formulation of dynamic properties of the dam are: 1) The dam is a linear elastic body with triangular cross sections, 2) shear distortion is predominant during vibration in the y direction which is concerned in this article, and 3) shear modulus distribution in the dam is expressed as

$$G = G_0 z \quad (1)$$

where z , G_0 and a are depth below the crest and constants, respectively, while mass density ρ is uniform within the dam.

From the above assumption 2), modal displacements relative to the foundation can be approximately represented by

$$v(x, z) - v(x, H_x) = f(x, z) \{ v(x, 0) - v(x, H_x) \} \quad (2)$$

where $v(x, 0)$ and $f(x, z)$ denote displacement of the crest and a modal shape along the height respectively. From the previous studies, the shape function $f(x, z)$ associated with Eq.(1) is given by

$$f(x, z) = c \psi^{-\nu} J_\nu(\psi) \quad (3)$$

where

$$\psi = \mu_m \left(\frac{z}{H_x} \right)^{\frac{2-a}{2}} \quad (4)$$

$$\nu = \frac{a}{2-a} \quad (5)$$

and $J_\nu(\psi)$ denotes Bessel function of first kind and order ν , u_m the m -th zero value of $J_\nu(\psi)$, H_x the cross sectional height, and c a normalizing constant. Fig. 2 shows the lowest two modal shapes ($m=1,2$) for several values of a .

Consider a prismatic finite element which is obtained by deviding the dam with respect to the x - z planes, as shown in Fig. 3. The element has four movable nodes, two of which (i and j) locate on the crest and others (s and t) at the base. Using local coordinates originating from the node i , the deflection along the crest is given by linear interpolation of deflections at nodes i and j .

$$v(x,0) = SCv_c \quad (6)$$

where

$$S = [1 \quad x] \quad (7)$$

$$C = \begin{bmatrix} 1 & 0 \\ -1/l & 1/l \end{bmatrix} \quad (8)$$

$$v_c = [v_i \quad v_j]^T \quad (9)$$

Similarly, the deflection at the base is interpolated as

$$v(x,H_x) = SCv_b \quad (10)$$

where

$$v_b = [v_s \quad v_t]^T \quad (11)$$

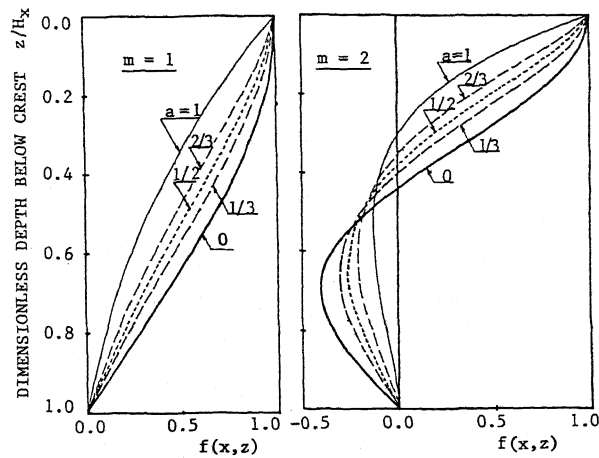


Fig. 2 Lowest Two Modal Shapes along Depth

Thus, the modal displacement at any point of the dam is given by

$$v(x,z) = SC\{f(x,z)v_c + [1-f(x,z)]v_b\} \quad (12)$$

Shear strain vector associated with the displacement in Eq.(12) is

$$\begin{aligned} \gamma &= [\gamma_{xy} \quad \gamma_{yz}]^T = [dv(x,z)/dx \quad dv(x,z)/dz]^T \\ &= BCv_c + PCv_b \end{aligned} \quad (13)$$

where

$$B = \begin{bmatrix} f_x(x,z) & f(x,z) + xf_x(x,z) \\ f_z(x,z) & xf_z(x,z) \end{bmatrix} \quad (14)$$

$$P = \begin{bmatrix} -f_x(x,z) & 1-f(x,z) - xf_x(x,z) \\ -f_z(x,z) & -xf_z(x,z) \end{bmatrix} \quad (15)$$

Shear stress vector related to the strain vector is

$$\tau = D \gamma \quad (16)$$

where

$$D = \begin{bmatrix} G & 0 \\ 0 & G \end{bmatrix} \quad (17)$$

The principle of virtual work applied to the element provides the stiffness and mass matrices expressed by

$$k = \begin{bmatrix} k_1 & k_2 \\ k_3 & k_4 \end{bmatrix} \quad (18)$$

$$m = \begin{bmatrix} m_1 & m_2 \\ m_3 & m_4 \end{bmatrix} \quad (19)$$

where

$$k_1 = \int_V C^T B^T D B C \, d(\text{vol}) \quad (20)$$

$$k_2 = k_3^T = \int_V C^T B^T D P C \, d(\text{vol}) \quad (21)$$

$$k_4 = \int_V C^T P^T D P C \, d(\text{vol}) \quad (22)$$

$$m_1 = \int_V \rho f^2(x, z) C^T S^T S C \, d(\text{vol}) \quad (23)$$

$$m_2 = m_3^T = \int_V \rho f(x, z) [1 - f(x, z)] C^T S^T S C \, d(\text{vol}) \quad (24)$$

$$m_4 = \int_V \rho [1 - f(x, z)]^2 C^T S^T S C \, d(\text{vol}) \quad (25)$$

Explicit forms of the above matrices are available in Apendices.

Simple Description of Foundation Properties

The simplest way to describe dynamic properties of ground underlying the dam is to establish parameters of a single degree of freedom (SDOF) system by which the ground is approximated. The parameters associated with horizontal vibration of a rectangular plate resting on an elastic half-space can be evaluated through knowledge of the dynamical ground compliance (Ref. 5). In a strict sense, the parameters evaluated from the dynamical ground compliance are frequency-dependent and adaptable only to a rigid plate. For the present purpose, however, they can be roughly regarded as independent of frequency, and also representative of properties averaged over a certain extent around a nodal point on the interface. With h and w denoting a half-length and a half width of a rectangular rigid plate, respectively, the parameters of the SDOF system are expressed as

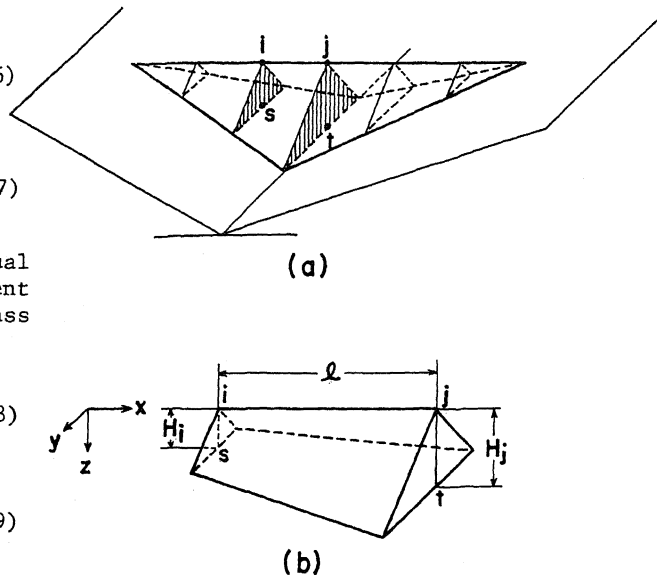


Fig. 3 Prismatic Finite Element of Dam

$$\text{spring constant} : k_f = 4.7(w/h)^{1/2} h G_f \quad (26)$$

$$\text{mass} : m_f = 0.37(w/h)^2 h^3 \rho_f \quad (27)$$

$$\text{damping constant} : c_f = 2.4(w/h) h^2 \sqrt{\rho_f G_f} \quad (28)$$

where a subscript f represents the foundation. The appropriate extent of the hypothetical rigid plate is determined by supposing both h and w, and comparing such analytical results as natural frequencies and modal shapes with those evaluated by the conventional method.

Structural matrices for the entire dam-foundation system can be obtained by assembling all the element matrices and foundation properties in an appropriate way.

ANALYTICAL EXAMPLES

Numerical analyses were done for two kinds of homogeneous earth dams, one located in rectangular canyons and the other in triangular canyons, changing a shear modulus ratio between the foundation

and dam. As for h and w in Eqs.(26)-(28), they were found to be related to the element length ℓ as well as to the shear modulus ratio G_f/G_d . In this study, they were set to $w=h=\ell/2$ for $G_f/G_d=100$ and 10, and $w=h/2=\ell$ for $G_f/G_d=3$ and 1. In Figs. 4 and 5 are shown the analytical results with respect to the fundamental mode of vibration. In Fig. 4 broken lines show the frequencies evaluated by the two dimensional finite element analysis (Ref. 4).

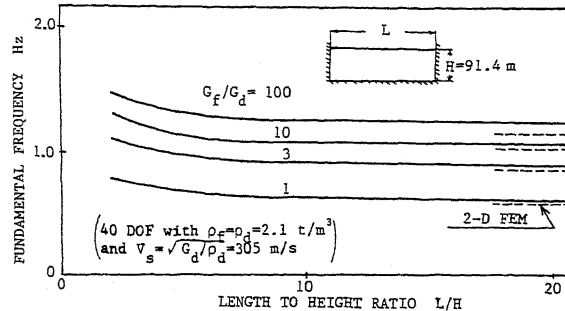


Fig. 4 Frequency of Dam with Rectangular Foundation

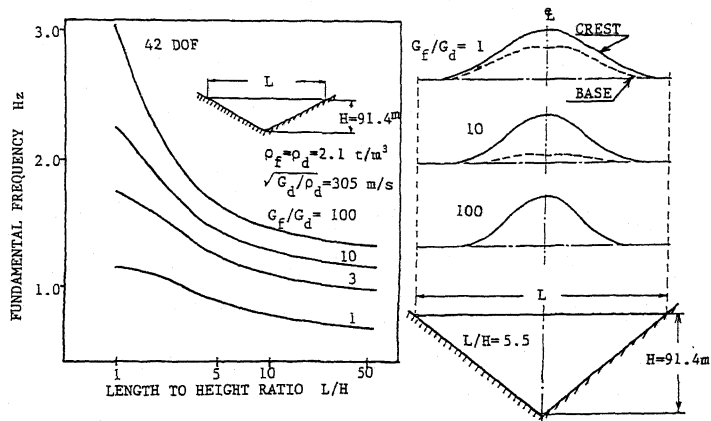


Fig. 5 Fundamental Vibration Mode of Dam with Triangular Foundation

CONCLUDING REMARKS

A simplified method has been presented for dynamic analysis of embankment dams with foundation interactions. Although the foundation treated in this article was supposed to be a uniform elastic medium, the method has advantage of being applicable to layered media only with a slight modification for Eqs.(26)-(28). Despite drastic simplification regarding a dam-foundation system, the authors believe that the method will serve one to draw many useful findings from actual dynamic interaction phenomena, and to estimate dynamic behaviors of the dam-foundation system during earthquakes.

APPENDICES

Explicit Representations of Element Matrices

To evaluate the volume integrals in Eqs.(20)-(22), it is convenient to express them as

$$k_1 = k_{1A} + k_{1B} + k_{1C} + k_{1D} \quad (A1)$$

$$k_2 = -k_1 + k_{2A} + k_{2B} \quad (A2)$$

$$k_4 = k_1 - 2k_{2A} - k_{4A} + k_{4B} \quad (A3)$$

where

$$k_{1A} = G_o b \int_0^l C^T N^T N C dx \int_0^{H_x} z^{a+1} f^2(x, z) dz \quad (A4)$$

$$k_{1B} = G_o b \int_0^l C^T (N^T S + S^T N) C dx \int_0^{H_x} z^{a+1} f(x, z) f_x(x, z) dz \quad (A5)$$

$$k_{1C} = G_o b \int_0^l C^T S^T S C dx \int_0^{H_x} z^{a+1} f_x^2(x, z) dz \quad (A6)$$

$$k_{1D} = G_o b \int_0^l C^T S^T S C dx \int_0^{H_x} z^{a+1} f_z^2(x, z) dz \quad (A7)$$

$$k_{2A} = G_o b \int_0^l C^T S^T N C dx \int_0^{H_x} z^{a+1} f(x, z) dz \quad (A8)$$

$$k_{2B} = G_o b \int_0^l C^T N^T N C dx \int_0^{H_x} z^{a+1} f_x(x, z) dz \quad (A9)$$

$$k_{4A} = G_o b \int_0^l C^T (N^T S + S^T N) C dx \int_0^{H_x} z^{a+1} f_x(x, z) dz \quad (A10)$$

$$k_{4B} = G_o b \int_0^l C^T N^T N C dx \int_0^{H_x} z^{a+1} dz \quad (A11)$$

in which b denotes a width to height ratio of the dam, and

$$N = [0 \quad 1] \quad (A12)$$

$m_1 = c^2 \frac{\rho b (\nu+1) l J_{\nu+1}^2(\mu_m)}{120 \mu_m^2} \begin{bmatrix} m_1^* & m_2^* \\ m_2^* & m_3^* \end{bmatrix}$ $m_2 = c \frac{(\nu+1) \rho b l}{120} \left\{ \frac{2 J_{\nu+1}(\mu_m)}{\mu_m^{\nu+1}} - \frac{c J_{\nu+1}^2(\mu_m)}{\mu_m^{2\nu}} \right\} \begin{bmatrix} m_1^* & m_2^* \\ m_2^* & m_3^* \end{bmatrix}$ $m_4 = \frac{\rho b l}{120} \left\{ 1 - \frac{4c(\nu+1) J_{\nu+1}(\mu_m)}{\mu_m^{\nu+1}} + \frac{c^2(\nu+1) J_{\nu+1}^2(\mu_m)}{\mu_m^{2\nu}} \right\} \begin{bmatrix} m_1^* & m_2^* \\ m_2^* & m_3^* \end{bmatrix}$	<p>where</p> $m_1^* = 12H_i^2 + 6H_i H_j + 2H_j^2$ $m_2^* = 3H_i^2 + 4H_i H_j + 3H_j^2$ $m_3^* = 2H_i^2 + 6H_i H_j + 12H_j^2$
---	---

Table A1 Explicit Element Mass Submatrices

$k_{1A} = c \frac{G_o b J_{\nu+1}^2(\mu_m)}{(a+2)(a+3)\rho\mu_m^{2\nu}} \begin{bmatrix} k_o^* & -k_o^* \\ -k_o^* & k_o^* \end{bmatrix}$	$k_{1B} = c \frac{G_o b J_{\nu+1}^2(\mu_m)}{(a+2)(a+3)\rho\mu_m^{2\nu}} \begin{bmatrix} (a+3)H_i^{a+2} - k_o^* & -\frac{(a+3)}{2}(H_i^{a+2} + H_j^{a+2}) + k_o^* \\ \text{sym.} & (a+3)H_j^{a+2} - k_o^* \end{bmatrix}$
$k_{1C} = c \frac{G_o b(\mu_m^2 + 4(\nu+1)^2)J_{\nu+1}^2(\mu_m)}{2(a+1)(a+2)(a+3)(\nu+1)(2\nu+3)\rho\mu_m^{2\nu}} \frac{1}{\Delta H} \begin{bmatrix} k_1^* & k_2^* \\ k_2^* & k_3^* \end{bmatrix}$	$k_{1D} = c \frac{G_o b \rho J_{\nu+1}^2(\mu_m)}{2(a+1)(a+2)(a+3)(\nu+1)\mu_m^{2\nu-2}(\Delta H)^3} \frac{1}{\Delta H} \begin{bmatrix} k_1^* & k_2^* \\ k_2^* & k_3^* \end{bmatrix}$
$k_{2A} = c \frac{G_o b(\nu+1)I_1}{(a+3)(a+4)\mu_m^{4\nu+2}(\Delta H)^2} \begin{bmatrix} k_4^* & -k_4^* \\ -k_5^* & k_5^* \end{bmatrix}$	<p>where $\Delta H = H_j - H_i$, and</p>
$k_{2B} = c \frac{G_o b I_2}{(a+2)\rho^2\mu_m^{4\nu+2}} (H_j^{a+2} - H_i^{a+2}) \begin{bmatrix} 1 & -1 \\ -1 & 1 \end{bmatrix}$	$k_o^* = (H_j^{a+3} - H_i^{a+3}) / \Delta H$
$k_{4A} = c \frac{G_o b I_2}{(a+2)(a+3)\mu_m^{4\nu+2}} \frac{1}{\Delta H} \begin{bmatrix} k_6^* & k_7^* \\ k_7^* & k_8^* \end{bmatrix}$	$k_1^* = -(a+1)(a+2)H_i^{a+3} + 2(a+1)(a+3)H_i^{a+2}H_j - (a+2)(a+3)H_i^{a+1}H_j^2 + 2H_j^{a+3}$
$k_{4B} = \frac{G_o b(\nu+1)}{2(2\nu+1)(a+3)\rho\mu_m^{4\nu+2}} \frac{H_j^{a+3} - H_i^{a+3}}{\Delta H} \begin{bmatrix} 1 & -1 \\ -1 & 1 \end{bmatrix}$	$k_2^* = -(a+1)H_i^{a+3} + (a+3)H_i^{a+2}H_j - (a+3)H_i^{a+1}H_j^2 + (a+1)H_j^{a+3}$
	$k_3^* = -2H_i^{a+3} + (a+2)(a+3)H_i^{a+1}H_j - 2(a+1)(a+3)H_i^{a+2}H_j + (a+1)(a+2)H_j^{a+3}$
	$k_4^* = -(a+3)H_i^{a+4} + (a+4)H_i^{a+3}H_j - H_j^{a+4}$
	$k_5^* = H_i^{a+4} - (a+4)H_i^{a+3}H_j + (a+3)H_j^{a+4}$
	$k_6^* = -2(a+2)H_i^{a+3} + 2(a+3)H_i^{a+2}H_j - 2H_j^{a+3}$
	$k_7^* = (a+1)H_i^{a+3} - (a+3)H_i^{a+2}H_j + (a+3)H_i^{a+1}H_j^2 - (a+1)H_j^{a+3}$
	$k_8^* = 2H_i^{a+3} - 2(a+3)H_i^{a+2}H_j + 2(a+2)H_j^{a+3}$
<p>Note: Values of I_1 for k_{2A} and I_2 for k_{2B} and k_{4A} are shown in Tab. A3 and Fig. A.</p>	

Table A2 Explicit Element Stiffness Submatrices

Substituting Eq.(3) into Eqs.(A4)-(A10) and integrating with respect to x and z , respectively, provide explicit forms of each submatrix. The integrals with respect to z in Eqs.(A4)-(A7) were analytically determined, while those in Eqs.(A8)-(A11) were numerically determined with the results shown in Table A3 and Fig. A in which I_1 and I_2 are

$$I_1 = \int_0^{H_x} z^{a+1} f(x,z) dz \quad (A13)$$

$$I_2 = \int_0^{H_x} z^{a+1} f_x(x,z) dz \quad (A14)$$

Explicit forms of the element stiffness submatrices are shown in Table A2, and those of the mass submatrices in Eqs.(23)-(25) are shown in Table A1.

ν	a	m	I_1	I_2
0	0	1	1.248460	2.497442
		2	-1.878288	-3.755761
1/5	1/3	1	1.848415	5.175086
		2	-5.968489	-16.72133
1/3	1/5	1	2.680104	8.938631
		2	-12.43695	-41.47649
1/2	2/3	1	4.683269	18.74315
		2	-31.49922	-125.9601
1	1	1	39.51253	237.1729
		2	-608.8475	-3655.191

Table A3 Several Examples of I_1 and I_2

References

- 1) Ohmachi, T.: Earthquake characteristics at dam foundations, Proc. Int. Symp. on Weak Rock, ISRM Tokyo Symp., Vol. 2, pp.1255-1260, 1981
- 2) Ohmachi, T. and Tokimatsu, K.: Simplified method for three-dimensional dynamic analysis of embankment dams, Proc. 4th Int. Conf. Num. Meth. Geomech., Vol. 1, pp.411-419, 1982
- 3) Ohmachi, T., Tokimatsu, K. and Soga, S.: Practical dynamic analyses of earth dams by a simplified 3-D method, Proc. 6th Japan Earthq. Engrng. Symp.-1982, pp.1145-1152, 1982
- 4) Chopra, A. K. and Perumalswami, P. R.: Dynamics of earthdams with foundation interactions, Jour. ASCE, EM2, pp.181-191, 1971
- 5) Kobori, T., Minai, R., Suzuki, T. and Kusakabe, K.: Dynamical ground compliance on a semi-infinite elastic medium (Part 1), Annual Report, Disaster Prevention Res. Inst., Kyoto Univ., No. 10A, pp.283-314, 1967

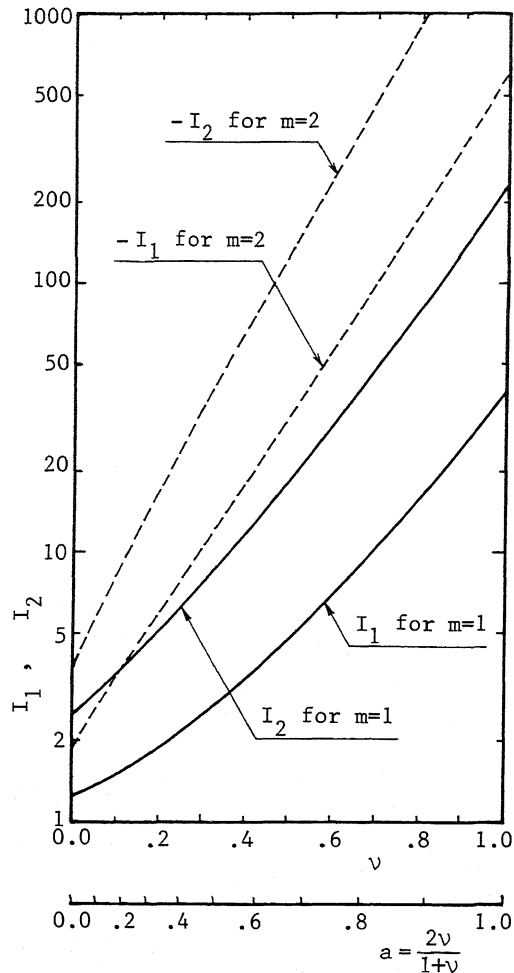


Fig. A Values of I_1 and I_2